New Methods for Horizon Line Detection in Infrared and Visible Sea Images

Ilan Lipschutz [1], Evgeny Gershikov[2] and Benjamin Milgrom[3]

Department of Electrical Engineering,
Braude Academic College of Engineering,

Abstract:

In this work we propose methods for horizon line detection and target marking in marine images captured by either infra-red (IR) or visible light cameras. A common method for horizon line detection is based on edge detection and the Hough transform. This method suffers from serious drawbacks when the horizon is not a clear enough straight line or there are other straight lines present in the image. We improve the algorithm performance by proposing a pre-processing stage eliminating some of the false detections. We also propose a new method for horizon line detection. The new algorithm is based on the idea of segmenting the image into two regions (sky and sea) by comparing the regional probability distribution functions (PDFs) or histograms. The line maximizing a statistical distance between these PDFs is chosen. This method is highly complex and can be further improved. Thus, we proceed to introduce two new methods combining the basic edge detection and Hough transform (EDHT) method to detect several candidate lines in the image and a statistical criterion to find the optimal line among the candidates. The chosen criterion can be based on regional covariances or the distance between PDFs as described above. We show that choosing the first option provides the best performance among the methods tested, at least with respect to the angular error, and yields a low complexity fast algorithm. We compare all the examined methods not only quantitatively by their average accuracy and relative speed, but also visually for several test images. Our conclusion is that all the methods introduced in this work can be beneficial for automatic processing of marine images for the purpose of tracking, navigation, target recognition and other applications.

Keywords: horizon detection, marine images, edge detection, Hough transform, image analysis, covariance based method, histogram-based method

1. Introduction

The horizon line is used for different purposes, such as navigation in airborne and marine vehicles and military surveillance. A number of horizon line detection methods are known, for example, [3-5, 7, 9-15]. Some of these methods are based on edge detection [8], while others employ different techniques [9]. Due to the variety of techniques, a comparison of the detection performance that they can achieve can be very helpful. The goal of this research is to take construct a robust, efficient and high performance algorithm for horizon line detection in both infrared and visible light images by introducing new techniques and combining them with existing methods. For simplicity, we consider methods that use only the luminance information of the image. Considering that in the later stages of this research the proposed algorithm is to be implemented on a stand-alone hardware unit, algorithms complexity and their relative speed is also evaluated.
First we examine some of the existing methods for sea-sky line detection that are of special interest in this work.

1.1. Edge detection and Hough transform based algorithm (H-EDHT)

The idea of using edge detection and the Hough transform [2] is not new. However, sometimes there are other strong edges present in the image that are confused for the horizon. We propose to use the pre-processing of Stages 1-3 to reduce the probability of this occurrence. The stages of this method can be summarized as follows.

[1] Pre-process the image using morphological erosion [15] to reduce the probability of the detection of weak edges in the later stages. A small circular structuring element can be used here. Alternatively, the image can be smoothed using a low pass filter, but we found erosion to provide better performance.

[2] In order to emphasize the horizon line and to decrease the non-relevant grayscale details we use standard deviation filtering [13] and mean filtering.

[3] An optional stage for clearing non-dominant lines: apply Canny's [1] edge detector to the mean filtered image, then logically invert the image bits and use morphological erosion similar to Stage 1 to thicken the image edge lines.

[4] Apply Canny's edge detector to the pre-processed image.

[5] Apply the Hough transform [2] to the edges map.

[6] Choose the horizon line to be the longest line found in the previous step.

226

1.2. Regional covariance based algorithm (H-COV)

An algorithm for horizon detection for remotely piloted micro air vehicles was introduced in [3]. The algorithm receives an image taken from the air as input and searches for an optimal partition of the image into two regions: sky and ground (or sky and sea) using a line, which is the detected horizon. The optimization criterion is based on the determinants and the traces of the covariance matrices of the two regions. More specifically, if we denote a sky pixel by $\boldsymbol{x}_{i,j}^{s} = [R_{i,j}^{s} \; G_{i,j}^{s} \; B_{i,j}^{s}]^{T}$, where $R_{i,j}^{s}, G_{i,j}^{s}, B_{i,j}^{s}$ are the primary red, green and blue values at the pixel (i,j) and, similarly, we denote a ground pixel by $\boldsymbol{x}_{i,j}^{g} = [R_{i,j}^{g} \; G_{i,j}^{g} \; B_{i,j}^{g}]^{T}$, then the covariance matrices of the regions are given by $\Lambda^{s} = E\left(\left(\boldsymbol{x}_{i,j}^{s} - \mu^{s}\right)\left(\boldsymbol{x}_{i,j}^{s} - \mu^{s}\right)^{T}\right)$, $\mu^{s} = E\left(\boldsymbol{x}_{i,j}^{s}\right)$ and $\Lambda^{g} = E\left(\left(\boldsymbol{x}_{i,j}^{g} - \mu^{g}\right)\left(\boldsymbol{x}_{i,j}^{g} - \mu^{g}\right)^{T}\right)$, $\mu^{g} = E\left(\boldsymbol{x}_{i,j}^{g}\right)$. E() denotes here statistical mean. The optimization criterion, considered for all the possible horizon line orientations and positions and maximized is given by:

$$(1) \quad J = \frac{1}{\det(\Lambda^{s}) + \det(\Lambda^{g}) + trace^{2}(\Lambda^{s}) + trace^{2}(\Lambda^{g})},$$

where det() denotes the determinant and trace() denotes the trace of the covariance matrices Λ^{s} and Λ^{g}.
We consider a similar criterion to the one in [3] for the luminance image, thus the optimization term J becomes

$$(2) \quad J = \frac{1}{\mathrm{var}(Y^{s}) + \mathrm{var}(Y^{g}) + \mathrm{var}^{2}(Y^{s}) + \mathrm{var}^{2}(Y^{g})},$$

where var() stands for variance and Y^{s}, Y^{g} are the luminance values of the sky and ground regions, respectively.
A simplified optimization criteria

$$(3) \quad J = \frac{1}{\mathrm{var}(Y^{s}) + \mathrm{var}(Y^{g})}$$

can be used instead of the one in [3] with similar results. Also, defining a region of interest (ROI) in the image and searching the horizon line only in this area speeds up the algorithm significantly. Alternatively, the input image can be down-sampled prior to the application of the algorithm to reduce its runtime, but this will decrease the accuracy as well.The structure of this paper is as follows. In the next section we present a new histogram based method for horizon line detection in marine images. Then in Section 3 we discuss algorithms combining the idea of edge detection and Hough transform with a statistical optimization criterion for determining the optimal line among a small set of candidates. In Section 4 we describe the methods and criteria used in the comparison of these algorithms and the horizon detection results: quantitative and visual. Section 5 presents a summary of this work and our conclusions.

2. A New Histogram Based Algorithm

The problem of finding the horizon line in sea images can be regarded as the problem of segmenting the image into two regions with different characteristics: the sky and the sea. We expect higher spatial correlations of the pixels inside each region than the inter-region correlations. This idea was exploited in Section 1.2 by calculating the covariance matrices in each region and maximizing a target function based on these matrices for all (or a set of) possible horizon line positions. Clearly, the target function is maximized when the covariance matrix of each region becomes closer to the matrix

$$(4) \quad CM = v \begin{pmatrix} 1 & 1 & 1 \\ 1 & 1 & 1 \\ 1 & 1 & 1 \end{pmatrix},$$

where v is a positive scalar, corresponding to the case of constant and equal red, blue and green values in each region. A distance metric between the sea and sky regions is not considered in Section 1.2, but can be added to the target function. For example, the terms $cov(R^{sky}, R^{sea})$, $cov(G^{sky}, G^{sea})$ and $cov(B^{sky}, B^{sea})$, standing for the covariances of the red, green and blue primary values, respectively, in the sky and sea regions, can be used. These covariances can be estimated using probability distributions or histograms of the image since usually the number of pixels in the two regions is not the same. Another idea is to measure the probability distribution functions (PDFs) in each of the regions and maximize the distance between those probability

227

functions. If the discrete PDF of the luminance in the sky region is denoted $p_Y^{Sky}(y)$ and the discrete PDF of the luminance in the sea region is denoted $p_Y^{Sea}(y)$ one can consider the Bhattacharyya distance between them, given by

$$(5) \quad D_B\left(p_Y^{Sky}, p_Y^{Sea}\right) = -ln\left(C_B\left(p_Y^{Sky}, p_Y^{Sea}\right)\right),$$

where C_B is the Bhattacharyya coefficient, calculated as

$$(6) \quad C_B\left(p_Y^{Sky}, p_Y^{Sea}\right) = \sum_y \sqrt{p_Y^{Sky}(y)\, p_Y^{Sea}(y)}.$$

We suggest maximizing the distance $D_B\left(p_Y^{Sky}, p_Y^{Sea}\right)$ or equivalently minimizing the coefficient $C_B\left(p_Y^{Sky}, p_Y^{Sea}\right)$ for a set of possible horizon line positions. One can also consider the Hellinger distance between the two PDFs, given by

$$(7) \quad D_H\left(p_Y^{Sky}, p_Y^{Sea}\right) = \sqrt{\frac{\sum_y \left(\sqrt{p_Y^{Sky}(y)} - \sqrt{p_Y^{Sea}(y)}\right)^2}{2}}$$

and related to the Bhattacharyya coefficient by

$$(8) \quad D_H\left(p_Y^{Sky}, p_Y^{Sea}\right) = \sqrt{1 - C_B\left(p_Y^{Sky}, p_Y^{Sea}\right)}.$$

Thus, maximizing the Hellinger distance or the Bhattacharyya distance is equivalent. Of course, other statistical distances for discrete PDFs can be considered as well. One could just replace the $D_B\left(p_Y^{Sky}, p_Y^{Sea}\right)$ distance below with any other suitable statistical distance. Note that it does not have to be a metric. We denote the algorithm H-HIS (HIS stands for Histograms) and propose the following steps.

2.1. Stages of the algorithm
The horizon line spatial and angular position can be measured by its height above the center of the image and its angle relative to the horizontal line going from left to right.
For all possible heights and angles of the line, that are considered, the following stages are to be performed.
[1] Segment the image using the line into two regions: sky and sea.
[2] Calculate the PDFs of both regions p_Y^{Sky} and p_Y^{Sea} using the same number of gray levels, e.g., 64 for color depth of 8 bits per pixel (for the luminance component or each of the primary colors).
[3] Calculate the Bhattacharyya distance D_B between the two histograms.

The line height and angle chosen are those corresponding to the maximum of $D_B\left(p_Y^{Sky}, p_Y^{Sea}\right)$.

3. Improving The H-Edht Algorithm
The H-EDHT algorithm, described above, can be improved by combining it with the H-COV or H-HIS algorithms. The idea is that after the stages of pre-processing and edge detection, instead of just choosing the longest line in the edge map, several candidate lines are considered among the longest ones. Then the line yielding the best segmentation of the image into sky and sea regions among the candidates is taken. The criterion of optimality here can be the one proposed for H-COV or the one proposed for H-HIS. Thus, we consider three algorithms following the same first stages until the edge map is produced and a predefined number (e.g., 5 or 10) of the longest candidate lines is taken. Then we can do one of the following.
a. Choose the candidate line having the maximal length. This is the basic H-EDHT algorithm.
b. Choose the candidate line providing the best segmentation of the image into sky and sea regions. The best segmentation is determined based on the maximal value of the criterion function of (3). We denote this algorithm H-EDHT-COV.
c. Once again we consider the best segmentation into two regions, but the criterion of optimality is that of (5). We denote this algorithm H-EDHT-HIS.

4. Comparison Methods And Results
Next, we describe the images and criteria used for the comparison of the algorithms described in this work.

4.1. Images used to compare the algorithms

The results of horizon detection for a group of 10 marine infra-red images and 10 marine visible light images are presented in this work. Image input format is true color (24 bit per pixel) non-compressed BMP. Resolutions used vary from around 300x200 to 1024x768 pixels. Most images contain a horizon line separating the sea and the sky clearly distinguished by the human eye. However, sometimes the horizon line is slightly distorted by camera optics and sea waves or concealed by marine vessels. To further challenge the selected algorithms, several images contained clouds or sun light effects near the surface of the sea water.

4.2. Comparison criteria

The algorithms were compared with respect to accuracy and speed. The accuracy was measured for the detected horizon angle (in degrees) relative to a horizontal line as well as the height of the line above the center of the image (in pixels). The errors provided in the next section for these two horizon line parameters are measured relative to the line height and angle as determined visually. The algorithms' speed was measured in terms of run time.

4.3. Quantitative results

The accuracy comparison for the algorithms described above (height and angle deviations) is given in Table 1 for infra-red images and in Table 2 for visible light images. In some of these images the horizon is not horizontally aligned (e.g., Figs. 1-3). As can be seen, the angular deviation is very small on average for the H-EDHT algorithms and especially H-EDHT-COV (0.06 degrees on average for IR images, 0.21 degrees for visible light images). The height deviation is smallest for the H-EDHT-COV method as well when considering IR images, but for visible light images, the best performers are H-COV and H-HIS. The run times of the methods are shown in Tables 3 and 4, as measured for a combined C++ and MATLAB implementation. When considering these results, the fastest technique is H-EDHT for both sizes of the images tested, but the H-EDHT-COV and H-EDHT-HIS methods are very close behind. The H-COV and H-HIS algorithms are significantly slower than H-EDHT due to the required intense computations of covariances or histograms in the process of the horizon detection.

4.4. Visual results

Visual results are provided in Figs. 1-2 for IR images and in Figs. 3-5 for visible light images. As can be seen, all the methods provide good results, however sometimes a small deviation can be observed from the horizon line as detected by the eye. Examples are H-COV result for IR_5 image (Fig. 1) or for IR_6 image (Fig. 2).

**Table 1. Mean height deviation (pixels) and angle deviation (degrees)
for the five algorithms when tested on IR images**

Algorithm	Mean height deviation	Mean angle deviation
H-EDHT	1.49	0.14
H-COV	2.63	0.42
H-HIS	2.90	0.72
H-EDHT-COV	0.65	0.06
H-EDHT-HIS	1.41	0.15

**Table 2. Mean height deviation (pixels) and angle deviation (degrees)
for the five algorithms when tested on visible light images**

Algorithm	Mean height deviation	Mean angle deviation
H-EDHT	3.69	0.28
H-COV	2.20	0.32
H-HIS	2.22	0.31
H-EDHT-COV	3.32	0.21
H-EDHT-HIS	3.25	0.24

229

Table 3. Mean run times (seconds) for the five horizon detection algorithms for images of size 640x480 [pixels]

Algorithm	Mean Time (sec.)
H-EDHT	0.2
H-COV	12.1
H-HIS	10.2
H-EDHT-COV	0.2
H-EDHT-HIS	0.2

Table 4. Mean run times (seconds) for the five horizon detection algorithms for images of size 1024x768 [pixels]

Algorithm	Mean Time (sec.)
H-EDHT	0.3
H-COV	61.1
H-HIS	48.9
H-EDHT-COV	0.4
H-EDHT-HIS	0.4

5. Conclusions

In this work we have compared five algorithms for automatic detection of the horizon line in marine images. These five algorithms include a method based on edge detection and Hough transform (H-EDHT), a covariance based method (H-COV), a new histogram based method (H-HIS) and two combinations of H-EDHT with the latter algorithms: H-EDHT-COV and H-EDHT-HIS. The H-EDHT method is commonly used for horizon line detection, but in this work we have added an improved pre-processing stage to it to enhance its performance, that includes the removal of noise and other obstructing details (like waves) from the image using morphological operations and other techniques. All five methods were implemented and tested on a group of infra-red images taken at night and on a group of visible light images taken during the day. We compared the algorithms with respect to angle and height deviations of the detected horizon line from the one determined manually and also with respect to run times. Our conclusion is that the H-EDHT-COV method is the most accurate algorithm with respect to the angle deviation, but it is sometimes less precise that H-COV or H-HIS with respect to the height deviation. If we consider the run times as well, the EDHT methods (H-EDHT, H-EDHT-COV and H-EDHT-HIS) are much faster than the covariance based H-COV or histogram based H-HIS algorithms. Thus, in applications were run-time is of primary importance, such as in real-time surveillance, we recommend using H-EDHT-COV, while for other applications H-COV can be a good candidate. All the methods, however, provide sufficiently good visual results. Note, that all the methods considered in this work use only the luminance information of the image for simplicity and low complexity of the algorithms. In the future, we intend to examine the use of the color information in visible light images [6] and determine whether it can improve the accuracy of horizon line detection.
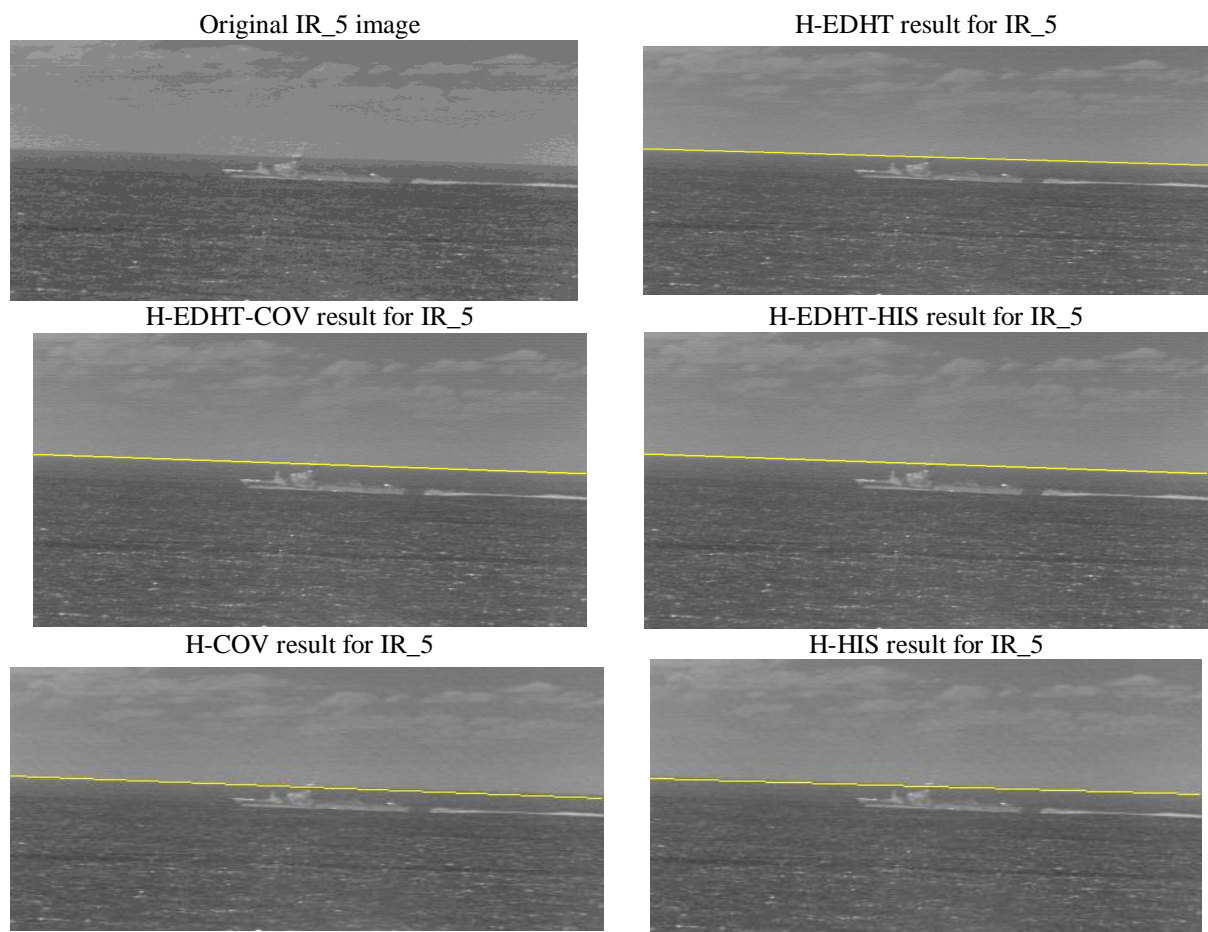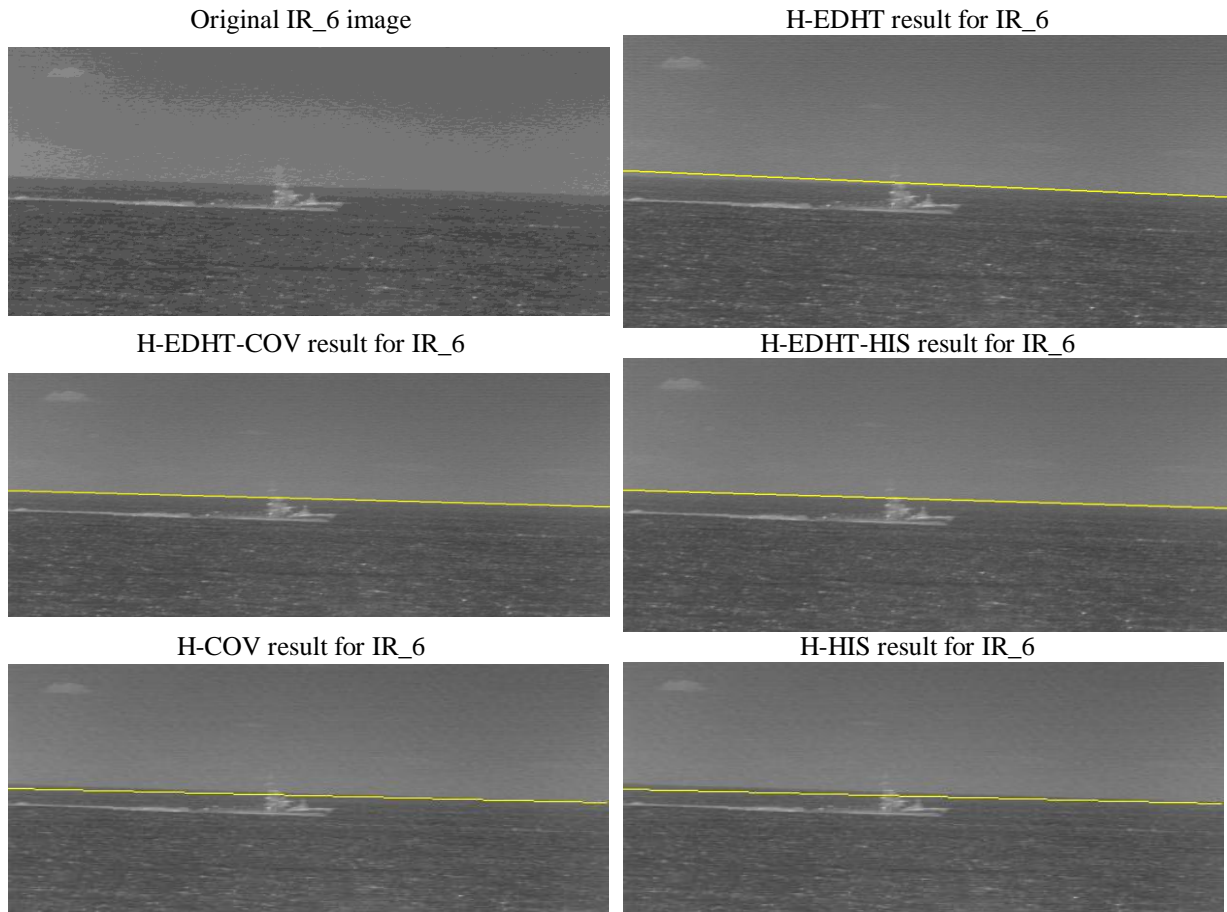
6. Acknowledgement

References

[1] J. Canny, "A computational approach to edge detection", IEEE Transactions on PAMI, 8(6), 1986, pp. 679-697.
[2] R. O. Duda and P. E. Hart, "Use of the Hough Transformation to Detect Lines and Curves in Pictures", Comm. ACM, 15(1), 1972, pp. 11–15.
[3] S. M. Ettinger, M. C. Nechyba, P. G. Ifju, and M. Waszak, "Vision-guided flight stability and control for micro air vehicles", Proc. IEEE Conf. on Intelligent Robots and Systems, Lausanne, Switzerland, 2002, pp. 2134 – 2140.
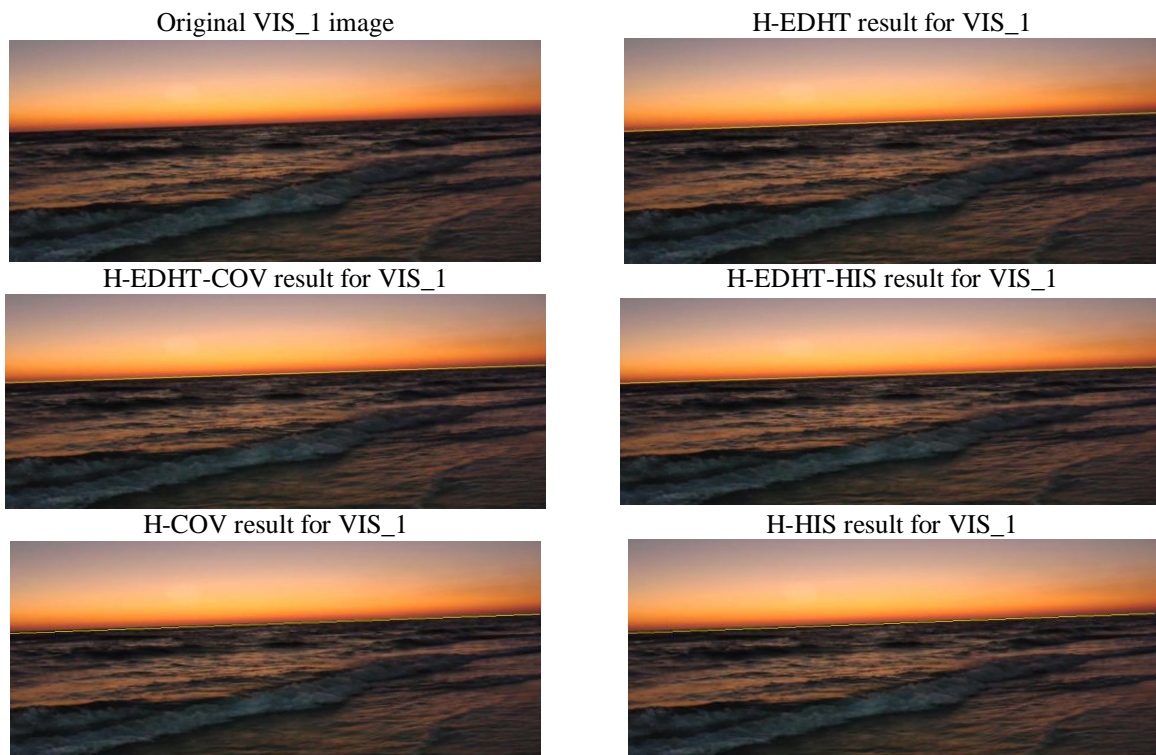
230

[4]   S. Fefilatyev, V. Smarodzinava, L.O. Hall, and D.B. Goldgof, "Horizon detection using machine learning techniques". Proc. Intern. Conf. on Machine Learning and App., 2006, pp. 17-21.

[5]   S. Fefilatyev, D.B. Goldgof, and L. Langebrake. "Towards detection of marine vehicles on horizon from buoy camera". Proc. SPIE, 2007, pp. 6736:67360O.

[6]   E. Gershikov and M. Porat, "On color transforms and bit allocation for optimal subband image compression", Signal Processing: Image Communication, 22(1), Jan. 2007, pp. 1-18.

[7]   C. Jiang, H. Jiang, C. Zhang and J. Wang; , "A New Method of Sea-Sky-Line Detection," Proc. of International Symposium on Intelligent Information Technology and Security Informatics (IITSI), April 2010, pp.740-743.

[8]   S. Kosolapov, "Robust Algorithms Sequence for Structured Light 3D Scanner Adapted for Human Foot 3D Imaging", Journal of Comm. and Computer, 8(7), 2011, pp. 595-598.

[9]   Tz. Libe, E. Gershikov and S. Kosolapov, "Comparison of methods for horizon line detection in sea images", Proc. CONTENT 2012, Nice, France, 2012, pp 79-85.

[10]   J.-W. Lu, Y.-Z. Dong, X.-H. Yuan and F.-L. Lu, "An algorithm for locating sky-sea line", Proc. of IEEE International Conference on Automation Science and Engineering, Oct. 2006, pp.615-619.

[11]   K. Nonami, F. Kendoul, S. Suzuki, W. Wang, and D. Nakazawa, Autonomous flying robots (Springer, Tokyo, Dordrecht, Heidelberg, London, New York, 2010).

[12]   Y. Wang, Z. Liao, H. Guo, T. Liu, and Y. Yang, "An approach for horizon extraction in ocean observation", Proc. IEEE Congress on Image and Signal Processing, 2009, Tianjin, China, pp. 1-5.

[13]   P. Wang, J. Tian and C. Gao, "Locating sea-sky line in infrared image based on complexed degree calculation", Proc. SPIE 7494, 74941P, 2009.

[14]   X. Wang, T. Zhang, L. Yan, X. Yang and G. Ao, "A method of sea-sky-line detection in complex sea background", Proc. SPIE 7495, 74950U, 2009.

[15]   D. Yan-zhi, S. Xiao-dong, W. Changjing, and X. Wei-gang, "Application of soft mathematical morphology in image segmentation of IR ship images", Proceedings ICSP 04, 2004, pp. 729-732.
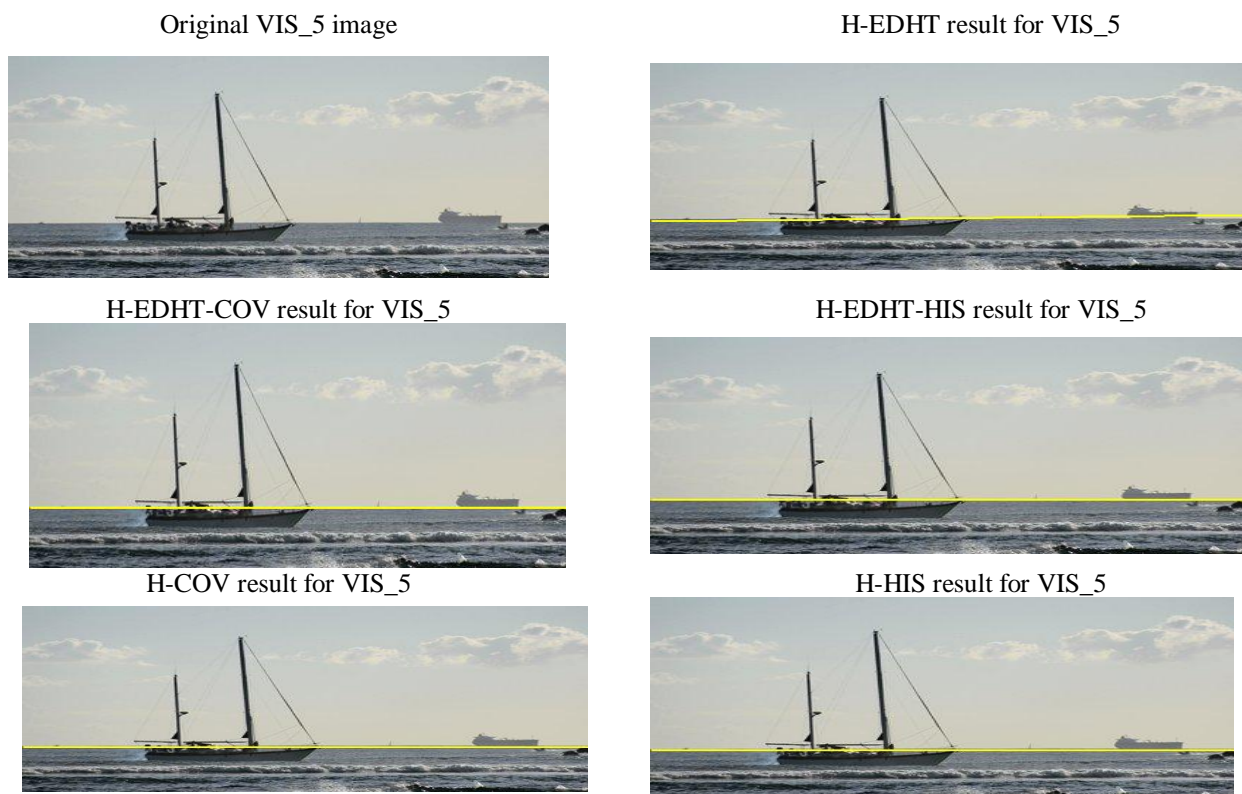
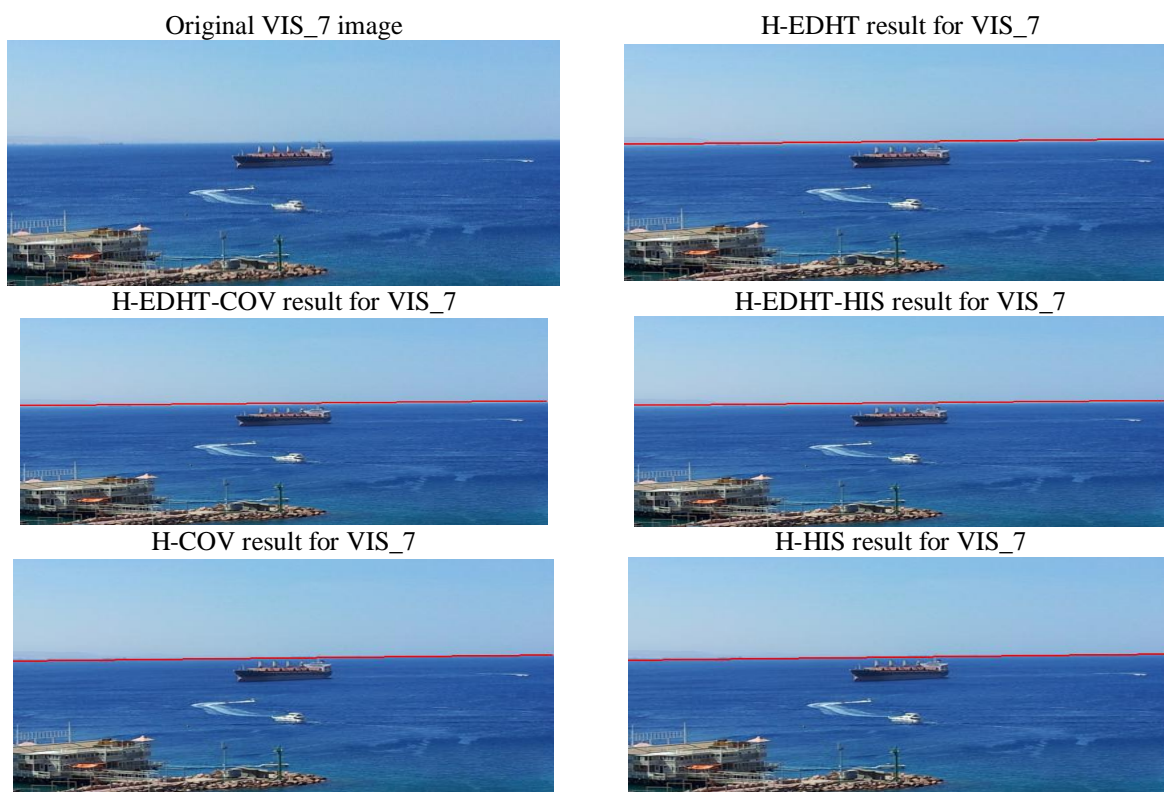Figure 1. Horizon detection results for image IR_5. The (yellow) line marks the detected horizon.

231

Original IR_6 image

H-EDHT result for IR_6

H-EDHT-COV result for IR_6

H-EDHT-HIS result for IR_6

H-COV result for IR_6

H-HIS result for IR_6

Figure 2. Horizon detection results for image IR_6. The (yellow) line marks the detected horizon.

Original VIS_1 image

H-EDHT result for VIS_1

H-EDHT-COV result for VIS_1

H-EDHT-HIS result for VIS_1

H-COV result for VIS_1

H-HIS result for VIS_1

Figure 3. Horizon detection results for image VIS_1. The (yellow) line marks the detected horizon.

232

Original VIS_5 image

H-EDHT result for VIS_5

H-EDHT-COV result for VIS_5

H-EDHT-HIS result for VIS_5

H-COV result for VIS_5

H-HIS result for VIS_5

**Figure 4. Horizon detection results for image VIS_5. The (yellow) line marks the detected horizon.
Despite the waves and the ship present, all the algorithms detect the horizon correctly.**

Original VIS_7 image

H-EDHT result for VIS_7

H-EDHT-COV result for VIS_7

H-EDHT-HIS result for VIS_7

H-COV result for VIS_7

H-HIS result for VIS_7

**Figure 5. Horizon detection results for image VIS_7. The (red) line marks the detected horizon.
Despite the waves, the ships and the land objects, all the algorithms detect the horizon correctly.**

233